

Energy Probability Distribution Zeros: A Route to Study Phase Transitions

B. V. Costa,^{1,*} L. A. S. Mól,^{1,†} and J. C. S. Rocha^{2,‡}

¹*Laboratório de Simulação, Departamento de Física, ICEEx*

Universidade Federal de Minas Gerais, 31720-901 Belo Horizonte, Minas Gerais, Brazil

²*Departamento de Física, ICEB, Universidade Federal de Ouro Preto, 35400-000 Ouro Preto, Minas Gerais, Brazil*

(Dated: December 3, 2024)

In this work we present a method to study phase transitions based on the complex zeros of a polynomial with coefficients determined by the energy probability distribution. This is a general method that brings advantages over the conventional Fisher zeros approach since it does not require the knowledge of the full density of states and allows the obtention of essentially the same informations. Indeed, only the energy histogram at a given temperature is used, the polynomial degree can be safely reduced and the polynomial coefficients spans over a reduced range of values, facilitating the zeros finder task as compared to the Fisher zeros. The method was applied to the 2D Ising, Potts and XY models and to a homopolymer model, showing its power in determining the phase transition properties of systems with first, second and infinity order phase transitions as well as systems with multiple phase transitions. Our strategy can easily be adapted to any model, classical or quantum, once we are able to build the corresponding energy probability distribution.

PACS numbers: 05.70.Fh, 05.10.Ln

I. INTRODUCTION

The study of phase transitions are of particular interest due to its practical importance and theoretical richness. Its understanding is the holy grail of thermodynamics and has implications in almost all areas of physics. Unfortunately, only a few special cases are accessible to a complete analytical description. In face of that many approximated techniques devoted to obtain the critical parameters, like transition temperatures and exponents, were developed along the years. Mean field approximations and the renormalization group [1, 2] are two of those approaches which have set remarkable advances in the understanding of phase transitions. Yang and Lee [3] introduced an alternative way to look to phase transitions by using the concept of zeros of the partition function, that has shown to be a worthwhile ground to understand it. Considering the complex fugacity plane, they showed that the partition function zeros density contains all the relevant information about the thermodynamic system, in particular they showed that in the thermodynamic limit the density of zeros completely determine the critical behavior of the system. In 1964 Fisher [4] extended this idea to the complex temperature plane (Fisher zeros).

In parallel to that the use of numerical techniques like Molecular Dynamics, Spin Dynamics and Monte Carlo grew dramatically following the accelerated development of fast computers and mainly due to the development of new algorithms. Of particular importance are the works of Swendsen and Wang [5, 6] developed to reduce critical

slowing down in continuous transitions and multicanonical methods (MUCA) [7–11] developed to overcome the barrier between two coexisting phases in a first order transition. In addition, the use of histograms to obtain the density of states ($g(E)$) have achieved an inconceivable level of sophistication as compared to a few decades ago. This advance has made it possible to obtain reliable results for quantities as $g(E)$ in the entire energy range allowing a step forward in the description of phase transitions. The Broad Histogram [12, 13] and the Replica Exchange Wang-Landau [14, 15] are among the state of the art techniques leading those researches. Working together with finite size scaling it allows one to approach the thermodynamic limit in a systematic and efficient way.

In this paper we introduce a new, general and efficient method based on the energy probability distribution (EPD) conjugated with an analogue of the Fisher zeros expansion of the partition function to precisely determine the transition temperature and exponents of a given system. The method has shown to be robust to be successfully extended to any model and has great potential to evoke further rigorous developments in our understanding of phase transitions. In the following we first describe the Fisher’s zeros approach. Next we describe how it can be combined with the EPD to obtain the critical behavior of a system. We demonstrate the reliability of the method by comparing our calculations with exact results for the 2d Ising model [16]. Its power is also demonstrated by calculating the critical properties for the 3, 6 and 10 states 2d Potts models [17], the 2d anisotropic Heisenberg model (XY model) [18–21], and one elastic and flexible polymer model [22]. Consequently, we report all the most relevant types of transitions, since 6 and 10 states Potts models have a first order transition, 3 states Potts model has a second order transition and the XY model has an infinity order tran-

* Electronic mail: bvc@fisica.ufmg.br

† Electronic mail: lucasmol@fisica.ufmg.br

‡ Electronic mail: jcsrocha@iceb.ufop.br

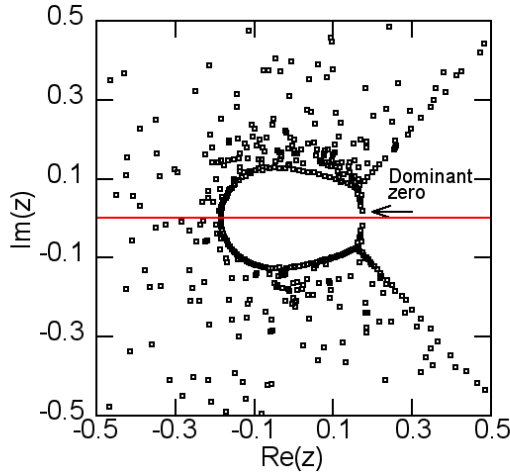


FIG. 1. Example of the Fisher zeros distribution for the Two Dimensional Ising Model. Here is shown for a 32×32 lattice. There are no zero in the real positive axis. The arrow marks the *dominant* zero. As the lattice size augments this zero converges to the real axis.

sition, also called Berezinskii-Kosterlitz-Thouless (BKT) transition [18, 19]. Besides that, the method has shown to be reliable to find all transitions in a richer system, for instance the 13 monomers polymer considered here. This polymer has two pseudo transitions, solid-globule and globule-coil, which can be identified as first and second order transitions respectively [23].

II. FISHER ZEROS

In the Fisher's zeros approach [4] a phase transition is characterized by the appearance of a zero in the positive real temperature axis in the thermodynamic limit reflecting the non-analyticity of thermodynamic functions in a phase transition. To make it clearer we should recall that the partition function is given by [24]

$$Z = \sum_{\mathbf{E}} g(\mathbf{E}) e^{-\beta \mathbf{E}} = e^{-\beta \varepsilon_0} \sum_n g_n e^{-\beta n \varepsilon}, \quad (1)$$

where $\beta = 1/k_B T$ is the inverse temperature and we assumed a discrete set of energies $\mathbf{E}_n = \varepsilon_0 + n\varepsilon$ with $n = 0, 1, 2, \dots$ [25]. This equation can be written as a polynomial in $z \equiv e^{-\varepsilon \beta}$ and factorized as

$$Z = e^{-\varepsilon_0 \beta} \prod_n (z - z_n). \quad (2)$$

For a finite system of volume L^d all zeros are complexes and we expect that some $\{z^*(L) = a(L) + ib(L)\} \in z_j(L)$, have the special property that $b(L) \rightarrow 0$ as $L \rightarrow \infty$ while $\lim_{L \rightarrow \infty} a(L) = a(\infty)$, a constant positive value, characterizing the phase transitions. To these zeros we will give the name dominant or leading zeros. In Fig. 1 it

is shown part of the z plane for the $2d$ Ising model zeros distribution. The identification of the dominant zero, generally the nearest zero to the real positive axis, is a way to locate the phase transition and determine the pseudo-critical temperature.

Although the exact density of states, $g(E)$, can be built exactly only in few exceptional cases, methods like *Wang-Landau* [14, 15] and *Multicanonical* [7–11] can give quite good estimates. The main problem concerning these methods is that in order to extract the relevant transition temperatures we have to build the entire map in the complex z plane, as discussed above, demanding one to construct the density of states in the whole energy range. For simple models and moderate system sizes this is not deterrent. However, as the volume of the system grows, the computer time needed to build $g(E)$ becomes prohibitive. Moreover, for larger volumes the number of energy states (the polynomial degree) increases dramatically, making the zeros finder task problematic. The density of states spans over many orders of magnitude, making it even worst. For instance, for a lattice size 96×96 in the $2d$ Ising model one has 9264 energy values and $g(E)$ spans over about 10^4 orders of magnitude. The smallest polynomial coefficient is $g(1) = 2$, the largest one is $g(4632) = 1.83 \times 10^{2772}$! At this point, one may be tempted to consider only the *most relevant* coefficients of the polynomial, probably the largest ones. However, these coefficients are generally related to very high energy states, unlikely to play any important role in the phase transition. Then, it should be interesting if we could “filter” the region where the dominant zero is located and still have the relevant information about the phase transition. This, in fact, can be done in a systematic way as we will show in the following.

III. ENERGY PROBABILITY DISTRIBUTION ZEROS

To introduce our method note that if we multiply Eq. 1 by $1 = e^{-\beta_0 \mathbf{E}} e^{\beta_0 \mathbf{E}}$ it can be rewritten as

$$Z_{\beta_0} = \sum_{\mathbf{E}} h_{\beta_0}(\mathbf{E}) e^{-\mathbf{E} \Delta \beta}, \quad (3)$$

where $h_{\beta_0}(\mathbf{E}) = g(\mathbf{E}) e^{-\beta_0 E}$ and $\Delta \beta = \beta - \beta_0$. Defining the variable $x = e^{-\varepsilon \Delta \beta}$ the partition function can be written as polynomial in the form

$$Z_{\beta_0} = e^{-\varepsilon_0 \Delta \beta} \sum_n h_{\beta_0}(n) x^n \quad (4)$$

where $h_{\beta_0}(n) = h_{\beta_0}(\mathbf{E}_n)$ is nothing but the non normalized canonical energy probability distribution (EPD), hereafter referred to as the energy histogram at temperature β_0 . The new polynomial has a new structure of zeros. Nevertheless, there is a one to one correspondence between the Fisher zeros and the EPD zeros since

they are related through a conformal transformation, although a detailed analysis of that is out of the scope of the present work.

Considering the histogram at the transition temperature, $\beta_0 = \beta_c$, the dominant zero will be at $x_c = 1$, i.e., $Z = 0$ at the critical temperature ($\Delta\beta = 0$) in the thermodynamic limit. For finite systems a small imaginary part of x_c is expected. Indeed, we may expect that the zero that signalizes a phase transition is the one with the smallest imaginary part on the real positive region regardless β_0 . Hence, one may find the critical temperature by locating it and using its distance to the point $(1, 0)$ to obtain $\Delta\beta$ and then estimate β_c .

With this in mind we have a clear criterion to filter the important region of the energy space where the most relevant zeros are located. For temperatures close enough to β_c only states with non-vanishing probability to occur are pertinent to the phase transition. Thus, for $\beta_0 \approx \beta_c$ we judiciously discard *small* values of h_{β_0} without introducing relevant deviations in x_c . This is the key aspect of our method. Now, we can safely work in a reduced energy range avoiding problems related to the sampling of the entire energy range and the zeros finder task for very high degree polynomials with coefficients spanning over many orders of magnitude.

We can carry out the precedent reasoning in the following way: We first build a normalized histogram $h_{\beta_0^0}$ ($\text{Max}(h_{\beta_0^0}) = 1$) at an initial guess β_0^0 considering a threshold for the coefficients as $h_{\beta_0^0} \geq 10^{-2}$ to reduce the energy range considered. Afterward, we construct the polynomial, Eq. 4, and perform the zeros finder task. As discussed before, by selecting the dominant zero, x_c^0 , we estimate the critical temperature, β_c^0 . Regarding that $\beta_c(L)$ is the true pseudo-critical temperature for the system of size L , if the initial guess β_0^0 is far from $\beta_c(L)$, presumably the estimative β_c^0 will not be satisfactory. Nevertheless, we can make $\beta_0^1 = \beta_c^0$, build a new histogram at this temperature and start over. After a *reasonable* number of iterations we may expect that β_c^j converges to the true $\beta_c(L)$ and thus x_c^j approaches the point $(1, 0)$. The property $x_c^j \rightarrow (1, 0)$ can be used as a consistency check in this iterative process. This suggests the following algorithm to find the pseudo-critical temperature:

1. Build a single histogram $h_{\beta_0^j}$ at β_0^j .
2. Find the zeros of the polynomial with coefficients given by $h_{\beta_0^j}$.
3. Find the dominant zero, x_c^j .
 - a) If x_c^j is close enough to the point $(1, 0)$, stop.
 - b) Else, make $\beta_0^{j+1} = -\frac{\ln(\Re\{x_c^j\})}{\varepsilon} + \beta_0^j$ and go back to 1.

IV. 2D ISING MODEL

The convergency and accuracy of the method can be

TABLE I. Estimate of the pseudo critical temperature for the ferromagnetic 2d Ising Model. The last line is the exact value up to five figures.

L	β	T	$ x $	$\Im m(x)$
4	0.6667	3.0000	0.6262	0.7652
	0.4504	2.2202	1.1130	1.2180
	0.4236	2.3607	0.9752	1.0939
	0.4299	2.3261	1.0059	1.1218
	0.4284	2.3343	0.9985	1.1150
	0.4288	2.3321	1.00045	1.1168
	0.4287	2.3326	0.9999	1.1159
8	0.4287	2.3326	0.9924	0.4241
	0.4306	2.3223	0.9999	0.4273
16	0.4306	2.3223	0.9923	0.2088
	0.4325	2.3121	0.9999	0.2104
32	0.4325	2.3121	0.9872	0.1035
	0.4357	2.2952	0.9998	0.1049
	0.43575	2.2949	0.9999	0.1049
64	0.43575	2.2949	0.9911	0.0520
	0.4380	2.2831	1.00005	0.0525
96	0.43575	2.2949	0.9967	0.0349
	0.4388	2.2789	0.9999	0.0350
estimate	0.4404	2.2707	-	-
∞	0.4407	2.2691	-	-

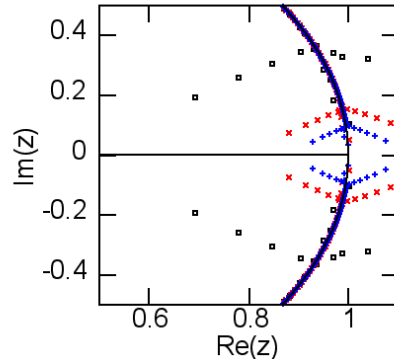


FIG. 2. Plot section of the zeros distribution for the Ising model. Lattices sizes are $L = 32, 64, 96$ (\square , \times and $+$ respectively.). The solid black line marks the perimeter of the unit circle and the real axis.

tested by using the 2d Ising model in a square lattice, which is defined by the following Hamiltonian:

$$H = -J \sum_{\langle i,j \rangle} \sigma_i \sigma_j, \quad (5)$$

where J is a ferromagnetic coupling constant, $\langle i,j \rangle$ means that the summation runs over nearest neighbors on a regular lattice and $\sigma_i = \pm 1$ is the spin variable at site i . As well known, this model has a continuous phase transition at $T_c = \frac{2}{\ln(1+\sqrt{2})} \frac{J}{k_B} \approx 2.269 \frac{J}{k_B}$ and was exactly solved in 1944 [16], being thus the preferred testing model

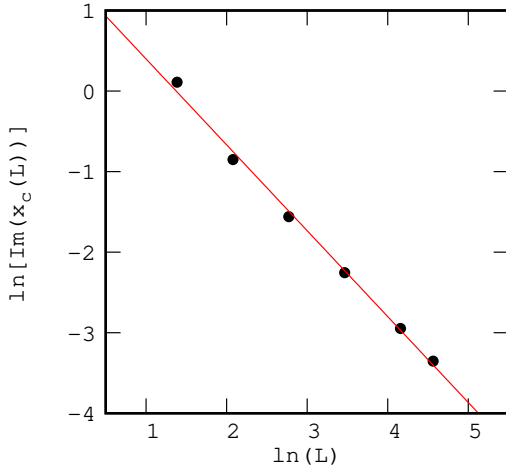


FIG. 3. Log-log plot of $\text{Im}(x_c(L))$ versus L for the Ising model. According to finite size scaling theory we expect the slope to be $1/\nu$. From our data we obtained $1/\nu = 1.07(3)$.

for new theories on phase transitions.

In Tab. I we show the results of the application of our method to the Ising model for several lattice sizes ($4 \leq L \leq 96$). For this we used the exact density of states calculated in Mathematica[®] using the code developed in Ref. 26 to build normalized histograms at selected temperatures. A threshold was introduced by searching for the minimum, E_{\min} , and maximum, E_{\max} , energy values for which the normalized histogram values are greater than 10^{-2} . The histogram values in the range $E_{\min} \leq E \leq E_{\max}$ were used as coefficients of a polynomial whose roots were calculated using the function *Solve* of Mathematica[®]. We show the critical temperature result of a finite size scaling (estimate entry) and the exact value up to 5 figures, showing an error smaller than 2%. The zeros distribution is shown in Fig. 2.

Other important quantity that can be readily obtained is the temperature critical exponent ν . As known [27], the finite size scaling theory predicts that $T_c(L) \sim T_c + aL^{-1/\nu}$ and thus, we might expect that $x_c(L) \sim x_c + bL^{-1/\nu}$. Once $\text{Re}\{x_c(L)\} \approx 1$, $\forall L$, the imaginary part of $x_c(L)$ should also scale as $L^{-1/\nu}$. Using this fact we can estimate in a log-log plot (see fig. 3) $1/\nu = 1.07(3)$, close to the exact value, 1. Of course, better results for T_c and ν can be obtained by diminishing the considered threshold, however, the energy range and consequently the polynomial degree increases, making the zeros find task more problematic and computationally more expensive, although not as complicated as in the Fisher zeros approach. Other source of error is the relatively small lattice sizes considered and possible corrections to scaling. A detailed analysis of the impact of the chosen threshold and finite size effects on results is in progress.

V. 2D POTTS MODEL

The q states Potts Model [17] is defined by the following Hamiltonian,

$$H = -J \sum_{\langle i,j \rangle} \delta_{\sigma_i, \sigma_j}, \quad (6)$$

where J is a ferromagnetic coupling constant, $\langle i,j \rangle$ means that the summation runs over nearest neighbors on a regular lattice, $\delta_{\alpha,\beta}$ is the Kronecker delta function ($\delta_{\alpha\beta} = 1$ if $\alpha = \beta$, 0 otherwise) and $\sigma_i = 1, 2, \dots, q$ is the spin variable at site i . In a square lattice it has a continuous (second order) phase transition for $q \leq 4$ and a discontinuous (first order) phase transition for $q > 4$ at $T_c = \frac{1}{\ln(1+\sqrt{q})} \frac{J}{k_B}$, where k_B is the Boltzmann constant. Hereafter we'll consider $J = 1$ and $k_B = 1$.

In order to test how our method performs with data from conventional Monte Carlo simulations we opted to work with the crudest possible implementation to see if it works even in the worst scenarios. Thus, we used conventional Metropolis sampling[28, 29] and single spin flips to study q states Potts models in a square lattice of linear size L ($N = L^2$ spins). Sites were chosen at random as well as the new spin value. One Monte Carlo Step (MCS) constitutes the attempt to assign a new value to N spins. No configuration was discarded after thermalization and then correlations between successive configurations are considerable. Also, no attempt to use cluster updates or any other optimized sampling was done, not even Heat-Bath sampling for high q [29]. The only quantity of interest in our simulations is the energy histogram, which is used to obtain the zeros. Then, after discarding N_{term} MCS for thermalization an energy histogram was built using N_{MCS} MCS and at the end of the simulation it was divided by its maximum value to give the normalized histogram used in the zeros calculation. Now, the threshold was introduced at 10^{-3} and zeros were calculated in the same way as for the Ising model. In what follows we detail the calculations for each q value studied.

A. 3 states

Initial scans for the critical temperature were done for $L = 20$ using $N_{\text{term}} = 50,000$ and $N_{\text{MCS}} = 500,000$ starting from $T_0^1 = 2.0, 1.0$ and 0.5 and after approximately 6 iterations the temperature converged to a value near $T_c(20) \approx 1.009$, as shown in fig. 4. This value was used as the initial temperature for another set of simulations from where critical temperatures were obtained. In this process an *ad hoc* diminishment of simulation temperature was employed for larger sizes. Table II shows detailed informations about simulation temperatures and parameters for each lattice size. In our process, after the first estimate of the critical temperature obtained by locating the zero with smallest imaginary part, single histogram reweighting [30] was used to obtain a new

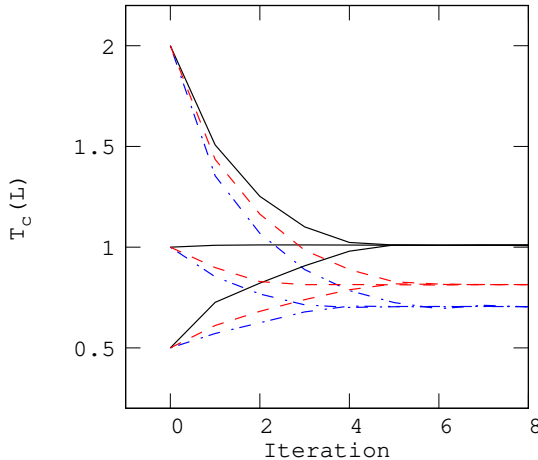


FIG. 4. Estimated critical temperature at each iteration for the 3 (full black lines), 6 (dashed red lines) and 10 (dotted-dashed blue lines) states Potts models for a $L = 20$ square lattice showing the fast convergence to the pseudo-critical temperature.

TABLE II. Monte Carlo parameters (N_{term} , N_{MCS} and T_{sim}) and results ($\Im m(\zeta_c(L))$ and $T_c(L)$) for the 3 states Potts model.

L	N_{term}	N_{MCS}	T_{sim}	$\Im m(\zeta_c(L))$	$T_c(L)$
20	10^5	5×10^6	1.0090	$5.151(9) \times 10^{-2}$	1.00978(3)
40	10^5	5×10^6	1.0000	$2.26(1) \times 10^{-2}$	1.0016(1)
60	3×10^5	5×10^6	0.9995	$1.42(2) \times 10^{-2}$	0.9992(1)
80	3×10^5	5×10^6	0.9970	$1.00(1) \times 10^{-2}$	0.9979(2)
120	3×10^5	5×10^6	0.9965	$6.157(5) \times 10^{-3}$	0.99663(5)
160	3×10^5	5×10^6	0.9960	$4.289(4) \times 10^{-3}$	0.9960(1)

histogram to generate the final set of zeros used to obtain final results shown in Table II. Errors were estimated by considering statistical fluctuations among 5 different Monte Carlo simulations for each lattice size.

In figs. 5 and 6 we show the finite size scaling analysis for the determination of the critical exponent and temperature respectively. In the first, a log-log plot of the imaginary part of the leading zero as a function of the lattice size gives an exponent $1/\nu = 1.19(1)$, in excellent agreement with the exact value[17] $6/5 = 1.2$. Using this value, we plotted $T_c(L)$ versus $L^{-1/\nu}$ which gives $T_c(\infty) = 0.99491(7)$, again, in excellent agreement with the exact value 0.99497.

B. 6 states

For the 6 states model we used the same approach. The main difference is that to obtain better results up to four simulations in temperatures slightly above and below the pseudo-critical temperature were used allowing better sampling near the weak first order transition.

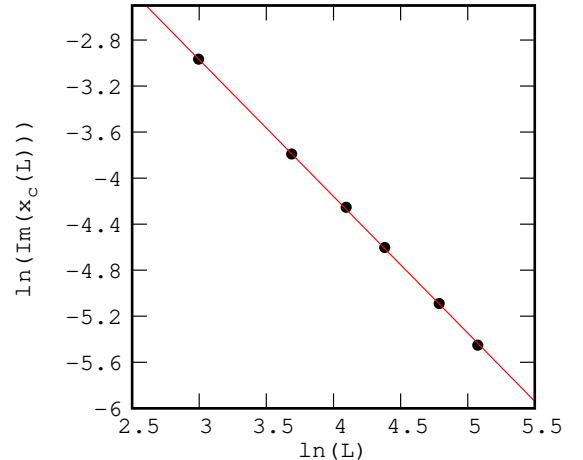


FIG. 5. Log-log plot of $\Im m(x_c(L))$ versus L for the 3 states Potts model. According to finite size scaling theory we expect the slope to be $1/\nu$. From our data we obtained $1/\nu = 1.19(1)$.

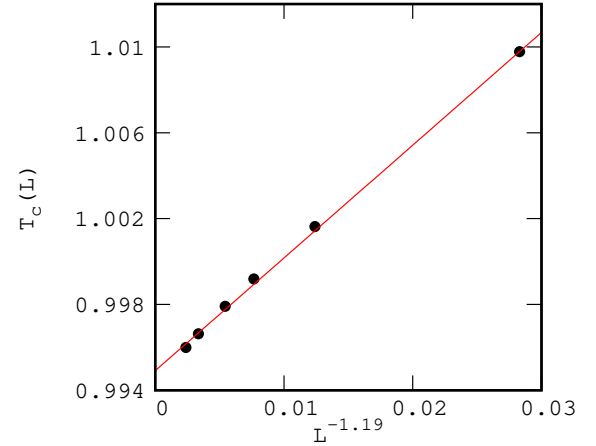


FIG. 6. $T_c(L)$ versus $L^{-1/\nu}$ for the 3 states Potts model. Extrapolation to thermodynamical limit ($L \rightarrow \infty$) gives $T_c(\infty) = 0.99491(7)$.

With these results, multiple histogram reweighting [31] was used to obtain the histograms from where zeros were calculated. As for the 3 states model two iterations were used to obtain final results. Table III shows detailed informations.

The finite size scaling in this case has shown to be more subtle. For this weak first order transition conventional finite size scaling functions with quantities depending on system volume[27] does give good enough results as shown by the solid lines in figs. 7 and 8 for the imaginary part of $x_c(L)$ and the pseudo-critical temperature respectively. However, when corrections to scaling are considered, i.e, by considering quantities depending on $aL^{-d} + bL^{-2d}$ instead of L^{-d} alone, the critical temperature encountered (0.80797(7)) agrees very well with the exact value (0.80761) besides the fact that this func-

TABLE III. Monte Carlo parameters (N_{term} , N_{MCS} and T_{sim}) and results ($\Im m(\zeta_c(L))$ and $T_c(L)$) for the 6 states Potts model.

L	N_{term}	N_{MCS}	T_{sim}	$\Im m(\zeta_c(L))$	$T_c(L)$
20	10^5	5×10^6	0.8100	0.2118(7)	0.814(2)
40	10^5	5×10^6	0.8100	0.669(3)	0.8098(8)
60	3×10^5	5×10^6	0.810		
	3×10^5	5×10^6	0.809		
	3×10^5	5×10^6	0.808	0.3387(8)	0.80880(5)
80	3×10^5	5×10^6	0.810		
	3×10^5	5×10^6	0.809		
	3×10^5	5×10^6	0.808	0.208(3)	0.8085(5)
120	3×10^5	5×10^6	0.810		
	3×10^5	5×10^6	0.809		
	3×10^5	5×10^6	0.808		
	3×10^5	5×10^6	0.807	0.109(3)	0.808(1)

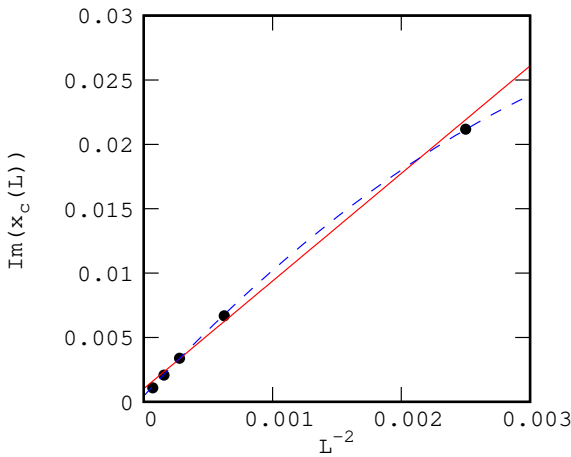


FIG. 7. $\Im m(x_c(L))$ versus L^{-2} for the 6 states Potts model. The solid red line is a linear adjust while dashed blue line is a quadratic fit. As can be seen the quadratic fit, i.e., when corrections to scaling are considered, the data are very well adjusted.

tion fits our points better than the pure L^{-d} function as shown by dashed lines in figs. 7 and 8.

C. 10 states

The 10 states Potts Model has a very strong first order phase transition[17]. Then, conventional sampling with Metropolis algorithm is not expected to give reliable results since the system has to cross a very high energy barrier to sample the low and high temperature states accordingly. Indeed, the energy barrier increases with increasing system size, making it even worst for larger systems. Thus, we opted to simulate small lattices ($L = 24, 28, 32, 36$) in such a way that both states are expected to be better sampled. For all simulations we used $N_{term} = 5 \times 10^5$ MCS, $N_{MCS} = 5 \times 10^6$ MCS and

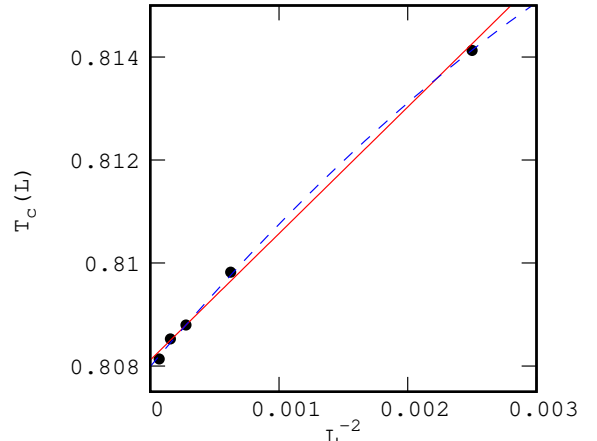


FIG. 8. $T_c(L)$ versus L^{-2} for the 6 states Potts model. Solid line is a linear adjust while dashed line is a quadratic fit. As can be seen the quadratic fit, i.e., when corrections to scaling are considered, the data are very well adjusted. From the adjust we get 0.80797(7).

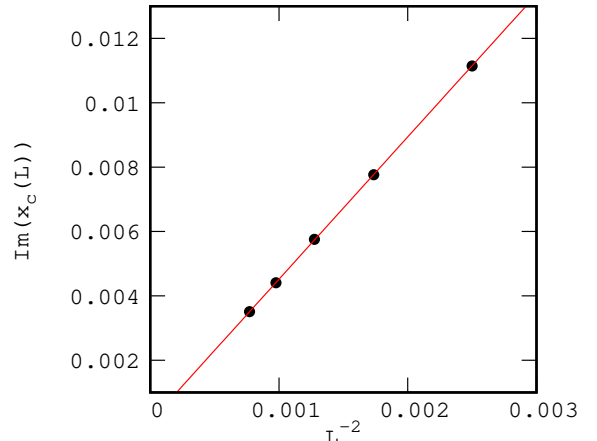


FIG. 9. $\Im m(x_c(L))$ versus L^{-2} for the 10 states Potts model. The solid line is a linear adjust showing excellent agreement with the predicted scaling law.

$T_0 = 0.725$ to get histograms. Single histogram reweighting was used to improve our results.

The finite size scaling analysis for the imaginary part of the zeros and for the critical temperature for the 10 states model is shown in figs. 9 and 10 respectively. As can be seen, even for these small lattice sizes corrections to scaling are negligible and the obtained critical temperature, 0.7014(8), is in excellent agreement with the exact value, 0.70123. The first order character of these transitions are evident from the double peak of histograms used to obtain the zeros, showing that our method is suitable for both, first and second order transitions.

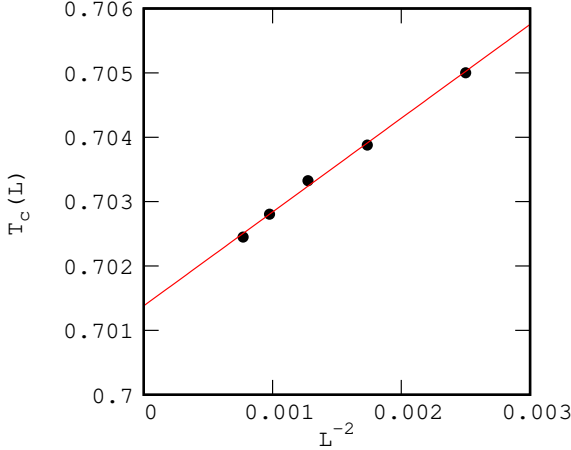


FIG. 10. $T_c(L)$ versus L^{-2} for the 10 states Potts model. The solid line is a linear adjust from which we get $T_c = 0.7014(8)$.

TABLE IV. Estimate of the BKT transition temperature for the XY Model.

L	$T_{BKT}(L)$
10	0.8491(1)
20	0.8049(5)
40	0.7755(6)
80	0.7536(4)
100	0.7587(2)
200	0.7364(3)
$\langle T_{BKT} \rangle$	0.7003(3)

VI. ANISOTROPIC HEISENBERG OR XY MODEL

Another test to our algorithm is the $2d$ anisotropic Heisenberg model, also known as XY model, which has a BKT transition [18, 19]. In this model the spin variable at site i is a classical 3D vector, $\vec{S}_i = (S_i^x, S_i^y, S_i^z)$, which interacts with neighbors by the following Hamiltonian:

$$H = -J \sum_{\langle i,j \rangle} \vec{S}_i \cdot \vec{S}_j. \quad (7)$$

Again, J is a ferromagnetic coupling constant and the summation runs over nearest neighbors. For these calculations, histograms were calculated from the density of states obtained by means of the Replica-Exchange-Wang-Landau algorithm[14, 15] whose details of implementation can be found on Ref. 25. This model has a continuum energy spectra and to overcome this we used a discretized energy set such that $E_n = n\varepsilon + \varepsilon_0$ [25, 32]. Only the final iteration results, averaged over 5 different simulations, are shown in Tab. IV. The last line is the result of the finite size scaling according to [33] $T_{BKT}(L) \sim [\ln(L)]^{-2}$ shown in fig. 11 which agree quite well with other estimates of the BKT temperature ($T_{BKT} \approx 0.700$ [20, 21, 25])

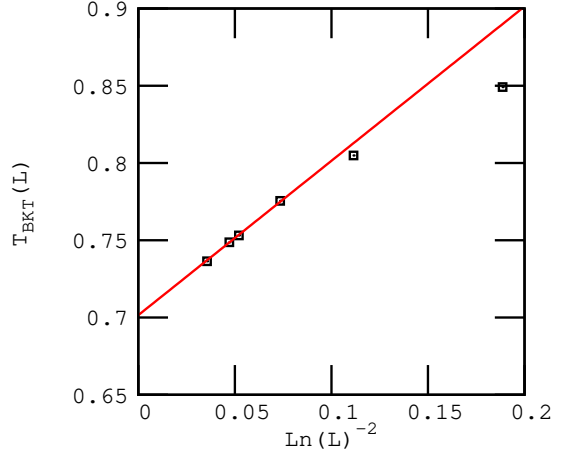


FIG. 11. $T_{BKT}(L)$ versus $1/\ln(L)^{-2}$ for the XY model. The solid line is a linear adjust from which we get $T_c = 0.7003(3)$. Small lattice sizes ($L = 10$ and 20) were not considered in the adjust.

VII. 13 MONOMER HOMOPOLYMER MODEL

As a final test to our algorithm we considered a 13 monomer flexible homopolymer, which is an intrinsically finite system with two pseudo-transitions, a first order one at $T_{1st} \approx 0.33520$ followed by a second order transition at $T_{2nd} \approx 1.1292$ [32]. In this model, we considered that unbounded monomers interacts by a truncated and shifted Lennard-Jones potential,

$$V_{LJ}^{mod}(r_{ij}) = V_{LJ}[\min(r_{ij}, r_c)] - V_{LJ}(r_c), \quad (8)$$

where r_{ij} is the distance between monomers i and j , r_c is the cutoff distance,

$$V_{LJ}(r) = 4\varepsilon \left[\left(\frac{\sigma}{r} \right)^{12} - \left(\frac{\sigma}{r} \right)^6 \right], \quad (9)$$

is the standard Lennard-Jones potential. We choose $\varepsilon = 1$, $\sigma = 2^{-1/6}r_0$ and $r_c = 2.5\sigma$. The elastic bonds between adjacent monomers is modeled by the finitely extensible nonlinear elastic (FENE) potential,

$$V_{FENE}(r_{i,i+1}) = -\frac{K}{2}R^2 \ln \left[1 - \left(\frac{r_{i,i+1} - r_0}{R} \right)^2 \right]. \quad (10)$$

This potential possesses a minimum at r_0 and diverges for $r \rightarrow r_0 \pm R$. K is a spring constant, and we set the parameters as $R = 0.3$, $r_0 = 0.7$, and $K = 40$.

The histograms were obtained from the density of states obtained by using the conventional Wang-Landau algorithm[14]. The flatness criteria was set to 0.7 and the final actualization factor was $\ln f = 10^{-9}$. Our results are in complete accordance with those obtained in Ref. [32] and are depicted in Tab. V. It is noteworthy that if we start the iteration at $T_0 > T_{2nd}$ or $T_0 < T_{1st}$

TABLE V. Determination of the transition temperatures for the 13 monomers elastic and flexible polymer. Two transitions are found. A low temperature first order and a second at higher temperature. The transition temperatures are to be compared with those in Ref. [32].

L	β	T	$ x $	$\Im m(x)$
13	10.0000	0.10000	1.02230	0.02650
	6.60690	0.15140	1.01414	0.01660
	4.44675	0.22488	1.00855	0.00806
	3.13696	0.31878	1.00135	0.00502
	2.92940	0.34142	0.99965	0.00502
	2.98685	0.33520	1.00002	0.00502
13	0.8333	1.2000	0.99988	0.00425
	0.8487	1.1783	0.99991	0.00423
	0.8625	1.1594	0.99994	0.00421
	0.8717	1.1472	0.99996	0.00420
	0.8779	1.1391	0.99997	0.00420
	0.8825	1.1331	0.99998	0.00420
	0.8856	1.1292	0.99999	0.00419

they always converge to T_{2nd} or T_{1st} respectively. If we use an intermediate value it can converge to one or another. The borders of the basin of convergence were not studied in this work. The first order character of the transition at T_{1st} is evident in the double peak structure of the histogram.

VIII. CLOSING REMARKS

In summary, we introduced a novel method to study phase transitions based on the zeros of the energy prob-

ability distribution. The method has shown to be fully applicable to any model allowing accurate determination of the critical temperatures and exponent ν as shown by our results on the Ising, Potts, Heisenberg and polymer models. Also, transition temperatures for different kinds of transitions - continuous, first order and BKT - were successfully and accurately obtained in this work.

The main advantage of the method when compared to others is that it is iterative, so that the transition temperature can be approached at will. Beside that a full knowledge of the density of states is not required and the polynomial we build has a few roots with its coefficients' ranging in a civilized, narrow region, making the zeros finder task non-problematic in the present method. Other advantage of the method is that ambiguities in the determination of pseudo-critical temperatures existing in canonical analysis in intrinsically finite systems is removed as evidenced by the polymer model studied here. Of course, much work is needed to unleash the method in its full power. Indeed, rigorous results and further numerical developments exploring its details may turn it a standard approach in the study of phase transitions.

ACKNOWLEDGMENTS

The authors gratefully acknowledge partial financial support from CNPq and FAPEMIG.

[1] L. P. Kadanoff, *Journal of Statistical Physics* **137**, 777 (2009).
[2] M. E. Fisher, *Rev. Mod. Phys.* **70**, 653 (1998).
[3] C. N. Yang and T. D. Lee, *Phys. Rev.* **87**, 404 (1952).
[4] M. E. Fisher, in *Lectures in Theoretical Physics: Volume VII C - Statistical Physics, Weak Interactions, Field Theory : Lectures Delivered at the Summer Institute for Theoretical Physics, University of Colorado, Boulder, 1964*, v. 7, edited by W. Brittin (University of Colorado Press, Boulder, 1965).
[5] R. H. Swendsen and J.-S. Wang, *Phys. Rev. Lett.* **58**, 86 (1987).
[6] U. Wolff, *Phys. Rev. Lett.* **62**, 361 (1989).
[7] B. A. Berg and T. Neuhaus, *Physics Letters B* **267**, 249 (1991).
[8] B. A. Berg and T. Neuhaus, *Phys. Rev. Lett.* **68**, 9 (1992).
[9] J. Lee, *Phys. Rev. Lett.* **71**, 211 (1993).
[10] B. A. Berg, *Journal of Statistical Physics* **82**, 323 (1996).
[11] B. A. Berg, *Nuclear Physics B - Proceedings Supplements* **39**, 2M(1998), Taylor, P. P. Aung, and W. Paul, *Phys. Rev. E* **88**, 012604 (2013).
[12] de Oliveira, P. M.C., Penna, T. J.P., and Herrmann, H. J., *Eur. Phys. J. B* **1**, 205 (1998).
[13] de Oliveira, P. M.C., *Eur. Phys. J. B* **6**, 111 (1998).
[14] F. Wang and D. P. Landau, *Phys. Rev. Lett.* **86**, 2050 (2001).
[15] T. Vogel, Y. W. Li, T. Wüst, and D. P. Landau, *Phys. Rev. Lett.* **110**, 210603 (2013).
[16] L. Onsager, *Phys. Rev.* **65**, 117 (1944).
[17] F. Y. Wu, *Rev. Mod. Phys.* **54**, 235 (1982).
[18] V. L. Berezinskii, *Journal of Experimental and Theoretical Physics - JETP* **32**, 493 (1971).
[19] J. M. Kosterlitz and D. J. Thouless, *Journal of Physics C: Solid State Physics* **6**, 1181 (1973).
[20] H. G. Evertz and D. P. Landau, *Phys. Rev. B* **54**, 12302 (1996).
[21] B. Costa, P. Coura, and S. Leonel, *Physics Letters A* **377**, 1239 (2013).
[22] S. Schnabel, T. Vogel, M. Bachmann, and W. Janke, *Chemical Physics Letters* **476**, 201 (2009).
[23] S. Schnabel, D. T. Seaton, D. P. Landau, and M. Bachmann, *Phys. Rev. E* **84**, 011127 (2011).
[24] J. C. S. Rocha, L. A. S. Mól, and B. V. Costa, ArXiv e-prints (2015), arXiv:1507.02231 [cond-mat.stat-mech].
[25] P. D. Beale, *Phys. Rev. Lett.* **76**, 78 (1996).

- [27] V. Privman, *Finite Size Scaling and Numerical Simulation of Statistical Systems* (World Scientific, 1990).
- [28] N. Metropolis, A. W. Rosenbluth, M. N. Rosenbluth, A. H. Teller, and E. Teller, The Journal of Chemical Physics **21**, 1087 (1953).
- [29] D. Landau and K. Binder, *A Guide to Monte Carlo Simulations in Statistical Physics* (Cambridge University Press, New York, NY, USA, 2005).
- [30] A. M. Ferrenberg and R. H. Swendsen, Phys. Rev. Lett. **61**, 2635 (1988).
- [31] A. M. Ferrenberg and R. H. Swendsen, Phys. Rev. Lett. **63**, 1195 (1989).
- [32] J. C. S. Rocha, S. Schnabel, D. P. Landau, and M. Bachmann, Phys. Rev. E **90**, 022601 (2014).
- [33] R. Kenna and A. Irving, Physics Letters B **351**, 273 (1995).